Chapter 11
Time-Dependent Non-similarity

In the previous Part, it has already been seen that the concept of *similarity* is not particular to the space variables only but is also equally applicable to the time variable. Owing to the physical and mathematical meanings of similarity, the criterion of self-similarity in time for stretching/shrinking surfaces has been derived in Chap. 8. Interestingly, the spectrum of self-similar unsteady flows due to the stretching or shrinking surfaces is very limited which in turn signifies the diversity of the non-similar flows to the unsteady case. Even being a very restricted family, the self-similar unsteady flows have widely been studied in the literature, whereas the non-similar unsteady flows have not been investigated on such a large scale. The reason behind this is again the nature of governing non-similar equations which are in fact the partial differential equations as they usually are in the case of spatial non-similarity. It is, however, a matter of fact that the temporal non-similarity does not pose a severe challenge as does the spatial non-similarity. In most of the cases, it is too light to be resolvable analytically, because of the homotopy analysis method (HAM) or the other series methods, etc., with great accuracy. In numerical computations, the straightforward finite difference schemes work well without requiring the use of Newton's method for the subsequent linearization of the nonlinear difference equations as is utilized in the Keller-Box scheme. Gaussian elimination procedure serves sufficiently for the solution of so-obtained simultaneous difference equations. Such analytic or numerical techniques shall be utilized in the coming Sections by considering some particular types of the surface velocity.

11.1 Two-Dimensional Unsteady Non-similar Flows

The cases of two- and three-dimensional flows follow the same non-similar formulation. Therefore, the preference shall be given the two-dimensional flows because of their mathematical simplicity in comparison with the three-dimensional flows. In the unsteady flows, caused due to uniform stretching/shrinking of the

A. Mehmood, *Viscous Flows*, Mathematical Engineering,
DOI 10.1007/978-3-319-55432-7_11

continuous surfaces, the strength of mathematical difficulty in the non-similar flows depends mostly upon the nature of the wall velocity assumed. In Chap. 8, it was determined that the temporal similarity is admitted only for the linear stretching or shrinking of the sheet when the wall velocity is inversely proportional to t, i.e., $u_w = \frac{ax}{t}$ or $u_w = \frac{ax}{1+\gamma t}$. All other forms of the wall velocity yield non-similar flows. The other source of non-similarity in time is the auxiliary data, that is, the initial and the boundary conditions. In Chap. 8, it was also realized that for a well-posed problem, the initial condition (essentially) and at least one of the boundary conditions must coalesce in order to establish the self-similarity. If the auxiliary data do not allow any such coalescing, then the establishment of self-similarity is impossible. Thus, if the wall velocity does not follow the above-mentioned forms or the auxiliary data do not allow any coalescing of the initial and boundary condition(s), the similarity solution will never be permissible. In all such situations, the temporal non-similarity is deemed unavoidable.

Temporal non-similarity may occur in both the spatially self-similar and non-similar flows. In this Chapter, we shall, however, restrict ourselves to the case of spatially self-similar flows. In such flows, the original three variables (x, y, t) shall be reduced to two due to suitable mixing of the original variables. The reduction of variables, in two-dimensional flow, from three (x, y, t) to two may occur in two ways: If the new variable is constructed due to x and t of the form x/t, then the solutions are usually called *pseudo-steady*; and if the three variables (x, y, t) are reduced to two by any other way, then the solutions are called *semi-similar*. In all those cases, where the spatial similarity is admissible, the similarity variable η is already constructed due to y and x, thus allowing no combination of the form x/t for the new variable. In such flows, the governing unsteady problem is eventually transformed to a partial differential equation admitting self-similarity in x and y but no similarity in time. Such a solution falls into the above-mentioned category of semi-similar solutions. A simple example from this category is the unsteady Crane's flow where the flat sheet is started impulsively to be stretching linearly in x-direction. In this case, the governing equations are given in Eqs. (2.10) and (2.11) (with $w = 0$) and the initial and boundary conditions are of the form

$$\left.\begin{array}{l} \text{at } t \le 0: \ u = v = 0, \forall x, y \\ \text{at } t > 0: \ \left\{\begin{array}{l} u = ax, v = 0, \quad \text{at} \quad y = 0 \\ u = 0, \quad \text{at} \quad y = \infty \end{array}\right. \end{array}\right\}. \tag{11.1a}$$

Sometimes they are also casted into the form

$$\left.\begin{array}{l} \text{at } t < 0: \ u = v = 0, \ \forall\, x, y \\ \text{at } t \ge 0: \ \left\{\begin{array}{l} u = ax, \ v = 0, \quad \text{at} \quad y = 0 \\ u = 0, \quad \text{at } y = \infty \end{array}\right. \end{array}\right\} \tag{11.1b}$$

which in a limiting sense $t \to 0$ is equivalent to (11.1a), that is, $t \to 0^+, u \to ax; t \to 0^-, u \to 0$. However, Eq. (11.1a) will be considered in the

coming analysis. In Eq. (11.1a), the wall velocity shows linear stretching of the wall in x-direction for which the similarity variables are given due to (Chap. 6) by

$$\eta = \sqrt{\frac{a}{\nu}}y, \frac{u}{ax} = f'(\eta), \tag{11.2}$$

in the steady flow situation. These new variables completely eliminate the previous variables from the governing equation, thus reducing it to the self-similar form. The consideration of unsteadiness in this case makes the variable t to appear in the equation of motion. Now, if the wall velocity does follow the form given in Eq. (8.15), then the flow is self-similar while non-similar otherwise. The non-similar or semi-similar formulation of the problem considered in this Section requires a proper extension of the similarity transformations (11.2). Initially, such problems had been investigated due to two different formulations particular to the small time or large time situations. Finally, a unified transformation, valid for small time as well as large time, was introduced by Williams and Rhyne [1]. A thorough discussion on this issue is given in the following paragraph.

The literature available on unsteady flow past the surfaces of finite length is very much rich and authentic, because of the pioneering contributions of the legends of the boundary-layer theory, in comparison with the literature on impulsively started continuous surfaces. Since the history of unsteady flows, caused either due to impulsively started continuous bodies or the bodies of finite length, goes back to the classical Rayleigh's problem, in the Rayleigh's problem the flow is developed in a stationary fluid due to the impulsive (uniform) motion of the bounding wall due to which the vorticity transports from the moving wall to the ambient fluid with the passage of time. After a while, when sufficient time has elapsed, the flow becomes fully developed within a finite thin region near the wall beyond which the ambient situation persists without any change. Such a situation is usually referred to as the establishment of steady state. Because of the above illustration, the boundary-layer seems to grow in time, which actually the case is, and is given by $\delta_R \sim \sqrt{\nu t}$, thus providing a natural length scale to this flow. Such an availability of appropriate length scale makes it possible to construct the new similarity variable $\eta_R = y/\sqrt{\nu t}$ in order to transform the governing partial differential equation of the Rayleigh's problem to an equivalent ordinary differential equation.

On the other hand, an exact similarity solution to the steady two-dimensional case does also exist which is commonly known as the Blasius solution. How the normal length scale δ_R (of Rayleigh's problem) could be utilized in the Blasius flow which is steady in nature. In this case, the boundary-layer thickness develops in streamwise direction (by staying independent of time) due to the presence of external potential flow. Therefore, the time t in the expression of Rayleigh's boundary thickness δ_R could be replaced by x/u_{ref} by interpreting it as the time required by a fluid particle to reach a distance x. In this way, the length scale δ_R modifies to $\delta_{FS} \sim \sqrt{\frac{\nu x}{u_{\text{ref}}}}$ to be utilized in the construction of similarity variable $\eta_{FS} = y\sqrt{\frac{u_{\text{ref}}}{\nu x}}$ of this flow. In this case, u_{ref} denotes the external reference velocity

of the Blasius or the Falkner–Skan type. The subscripts R and FS are particular to the Rayleigh problem and the Falkner–Skan flow, respectively. Thus, in the case of two-dimensional unsteady flow over a finite plate, the Rayleigh's solution and the Blasius or Falkner–Skan solution serve as the initial and final solutions, respectively.

By utilizing the above-named initial and final solutions, the unsteady flow past a wedge has been formulated by several researchers. Because of the availability of similarity variables, that is, $\eta_R = y/\sqrt{\nu t}$ and $\eta_{FS} = y\sqrt{\frac{u_e}{\nu x}}$, two separate formulations have been developed referring to the small time and large time solutions. While doing so, the time has been non-dimensionalized as $\tau = \frac{u_{\text{ref}} t}{x}$. Because of the variables η_R and τ, the resulting formulation agrees well with the Rayleigh's solution for small time but does not match the Falkner–Skan solution for large time. Similarly, the formulation due to η_{FS} and τ fits very well to the Falkner–Skan solution for large τ but deviates from the Rayleigh's solution for small τ. The reason behind this fact is that the so-obtained non-similar equations change their character as τ increases (starting) from 0 and crosses the value $\tau = 1$. Consequently, the transformation serving appropriate for small τ diverges for large τ and the vice versa. This fact was first pointed out by Stewartson [2] in 1951. This issue was finally resolved by Williams & Rhyne [1] by determining a unified formulation which reduces to η_R and τ (formulation) for small τ and $\eta_{FS}\&\tau$ (formulation) for large τ. In doing so, the semi-infinite time domain of τ has been collapsed to closed interval $[0, 1]$ which in fact facilitates in the numerical integration of the governing equations. The new time variable constructed by Williams and Rhyne [1] is given by

$$\xi = 1 - \mathrm{e}^{-\frac{u_{\text{ref}} t}{x}},$$

according to which, $\xi \to 0$ as $\frac{u_{\text{ref}} t}{x} \to 0$ and $\xi \to 1$ as $\frac{u_{\text{ref}} t}{x} \to \infty$. Thus, the steady-state Falkner–Skan solution appears at the end of the new time interval $(\xi = 1)$, and the Rayleigh's solution is recovered at the start of the time interval, that is, at $\xi = 0$. For detailed derivation of such a semi-similar (non-similar) solution, the reader is referred to follow [1].

The transformation developed by Williams and Rhyne has frequently been used in the study of unsteady laminar flows over continuous surfaces or surfaces of finite length (see for instance [3–7] and the references there in). Thus, for the unsteady Crane's flow, the steady similarity transformations (11.2) extend to the semi-similar form as

$$\eta = \sqrt{\frac{a}{\nu\xi}}y,\ \psi = \sqrt{a\nu\xi}\, x f(\xi, \eta),\ \xi = 1 - \mathrm{e}^{-\tau};\ \tau = at, \tag{11.3}$$

due to which the equation of continuity is satisfied identically and the momentum equation takes the form

$$\xi\left(\left(\frac{\partial f}{\partial \eta}\right)^2 - f\frac{\partial^2 f}{\partial \eta^2}\right) = \frac{\partial^3 f}{\partial \eta^3} + \frac{1}{2}(1-\xi)\eta\frac{\partial^2 f}{\partial \eta^2} - \xi(1-\xi)\frac{\partial^2 f}{\partial \eta \partial \xi}, \tag{11.4}$$

subject to the boundary conditions

$$f(0,\xi) = 0, \left.\frac{\partial f}{\partial \eta}\right|_{\eta=0} = 1, \quad \text{and} \left.\frac{\partial f}{\partial \eta}\right|_{\eta=\infty} = 0. \tag{11.5}$$

Clearly, at $\xi = 0$, Eq. (11.4) recovers the Rayleigh's problem, and at $\xi = 1$, it reduces to the self-similar Crane's equation. As evident from their name, semi-similar, such flows do not depart far away from the self-similar solution. Only in a small neighborhood of $\xi = 0$, the solution undergoes temporal transition and finally achieves the steady-state self-similar solution corresponding to the large values of ξ. Because of this fact, the level of (mathematical) difficulty in these "non-similar" problems is not that severe as it is in the case of spatially non-similar problems. These problems can easily be solved by usual finite difference schemes. Asymptotic analytic solutions are also possible due to the conventional asymptotic expansion (in ξ) or due to the homotopy methods. The homotopy analysis method, in particular, works very well with these problems without taking enough long time or facing the issues of convergence. In contrast, the spatially non-similar equations are quite hard to solve with such asymptotic series solution methods such as HAM or HPM.

System (11.4) and (11.5) has been solved analytically due to HAM procedure, and the results have been depicted in Figs. 11.1 and 11.2. The velocity profile can be seen plotted against η at different values of the time variable ξ. For small values of ξ, transition from the Raleigh's solution to that of Crane's can be seen quite obvious upon increasing the values of ξ. For sufficiently large values of ξ, the flow is shown fully developed in the steady state with no further dependence upon time. The coefficient of wall skin-friction modifies in this case as

$$Re_x^{1/2} C_f = \xi^{-1/2}\left.\frac{\partial^2 f}{\partial \eta^2}\right|_{\eta=0}, \tag{11.6}$$

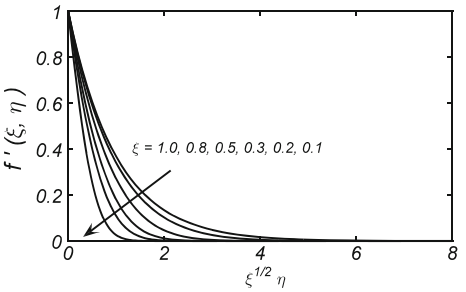

Fig. 11.1 Velocity profile against η for different ξ

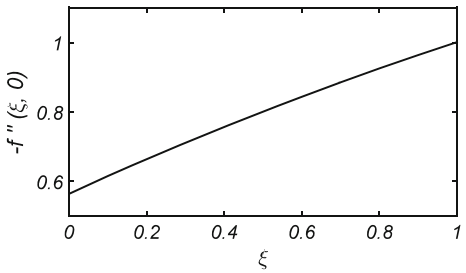

Fig. 11.2 Velocity gradient function at $\eta = 0$ plotted against ξ

where $Re_x = ax^2/v$ is the local Reynolds number. The values of $f''(\xi, 0)$ have been plotted in Fig. 11.2 where the wall velocity gradient can be seen increasing rapidly in the transition time period and stabilizing, afterward, for large values of time.

The same problem was first considered by Wang et al. [8] for the impulsively started stretching sheet. They utilized the usual similarity transformations introduced by Crane for the steady case (Eq. 11.2) and obtained an asymptotic solution for small and large time and a numerical solution as a whole. Their, so-reduced, semi-similar equation appeared in the form

$$\frac{\partial^2 f}{\partial \eta \partial \xi} + \left(\frac{\partial f}{\partial \eta}\right)^2 - f\frac{\partial^2 f}{\partial \eta^2} = \frac{\partial^3 f}{\partial \eta^3}, \tag{11.7}$$

which differs mainly, from Eq. (11.4), in the important Rayleigh's term (second term on the right-hand side). The first term on the left-hand side of Eq. (11.7) seems to stay dominant for small time values, but the contribution of the remaining two terms on the left-hand side, representing the convective acceleration, has also not been restricted to the large time values as has been done in Eq. (11.4). The basic reason behind this fact is the utilization of the transformation group $\eta_{FS}\&\tau$ as we explained previously. On the other hand, Pop and Na [9] also considered the same problem by utilizing the other similarity group, namely the $\eta_R\&\tau$. Consequently, they obtained an equation of form (11.4) with a bit different coefficient given by

$$4at\left(-f\frac{\partial^2 f}{\partial \eta^2} + \left(\frac{\partial f}{\partial \eta}\right)^2\right) = \frac{\partial^3 f}{\partial \eta^3} + 2\eta\frac{\partial^2 f}{\partial \eta^2} - 4t\frac{\partial^2 f}{\partial \eta \partial t}. \tag{11.8}$$

Clearly, for small values of time $(t \to 0)$, Eq. (11.8) recovers the Rayleigh's solution, but for large values of time, the last two terms on the right-hand side of Eq. (11.8) do not seem to vanish out in order to recover the Crane's solution. Thus, in order to find a solution which is uniformly valid for all time, the Williams & Rhyne's transformations (11.3) are observed to be the perfect choice.

11.1.1 Oscillatory Stretching of the Sheet

Continuing with the semi-similar solutions, there are several other forms of the wall velocities for which the resulting equations are semi-similar. A general criterion in this regard is the admissibility of spatial self-similarity by the problem. This can only be ensured when the spatial dependence of the wall velocity follows either the power-law or exponential form as derived in Chap. 5. The problem considered in the above discussion, namely the unsteady Crane's flow, follows the power-law wall velocity with an impulsive start. Another generalization of the Crane's flow is to take the oscillatory stretching rate of the uniform stretching velocity in the form

$$u_w(x,t) = (a\cos\omega t)x.$$

Such a wall velocity was considered by Wang [10] for which he utilized the similarity transformation of form (11.2) and introduced the dimensionless time of the form $\tau = \omega t$. In this case too, he obtained the transformed equation of form (11.7) given by

$$St\,\frac{\partial^2 f}{\partial\eta\partial\tau} + \left(\frac{\partial f}{\partial\eta}\right)^2 - f\frac{\partial^2 f}{\partial\eta^2} = \frac{\partial^3 f}{\partial\eta^3}, \tag{11.9}$$

with a perturbation parameter St representing the frequency of oscillations. The parameter St is defined as the ratio of oscillations' frequency to the amplitude of oscillations which is commonly referred as the Strouhal number, that is, $St = \omega/a$. Large values of St correspond to high-frequency oscillations with very small amplitude. Owing to the physical justification of this behavior, Wang obtained perturbation solution for large values of St. However, a quite exact analytic or numerical solution of Eq. (11.9) which is uniformly valid for small and large values of the Strouhal number is possible to obtain with the aid of commonly used HAM or finite difference schemes. Abbas et al. [11] considered sinusoidal oscillations in the stretching rate of a linearly stretching flat sheet immersed in a non-Newtonian viscoelastic fluid[1] under the influence of uniform magnetic field. They utilized the same transformations as did the Wang [10], that is, Eq. (11.2) by appending $\tau = \omega t$ to it and obtained the semi-similar system of the form

$$St\,\frac{\partial^2 f}{\partial\eta\partial\tau} + \left(\frac{\partial f}{\partial\eta}\right)^2 - f\frac{\partial^2 f}{\partial\eta^2} + M^2\frac{\partial f}{\partial\eta} = \frac{\partial^3 f}{\partial\eta^3} + K\left(s\frac{\partial^4 f}{\partial\eta^3\partial\tau} + 2\frac{\partial f}{\partial\eta}\frac{\partial^3 f}{\partial\eta^3} - \left(\frac{\partial^2 f}{\partial\eta^2}\right)^2 - f\frac{\partial^4 f}{\partial\eta^4}\right), \tag{11.10}$$

[1]The non-Newtonian fluids are not a topic of concern here. This problem has been chosen to report just because of the flow assumptions and solution procedure regardless of the nature of fluid.

subject to the boundary conditions

$$\left.\frac{\partial f}{\partial \eta}\right|_{\eta=0} = \sin\tau,\ f(0,\tau) = 0,\ \left.\frac{\partial f}{\partial \eta}\right|_{\eta=\infty} = 0,\ \left.\frac{\partial^2 f}{\partial \eta^2}\right|_{\eta=\infty} = 0. \tag{11.11}$$

Ignoring the physical nature of the parameters M, K and s, they have simply been considered as pure constants. The authors of [11] obtained a purely analytic solution to the system (11.10)–(11.11), with the aid of HAM, which is uniformly valid for small and large values of St. They also obtained an efficient numerical solution to the same system based on the finite difference scheme and reported a comparison of the two solutions. It is demonstrated (in [11]) that the analytic HAM solution produces sufficiently accurate approximation in order to meet the numerical one. A listing of numerical values of the skin-friction coefficient is given in Table 11.1 for various values of the involved physical parameters.

The problems presented under this head are though semi-similar but differ by a little in the level of difficulty from those considered in this Section prior to this head, corresponding to the impulsively started sheet. In such problems, the boundary conditions stay fixed and the time variable needs to be manipulated only in the governing equations, whereas, in the problems corresponding to the oscillatory rate of stretching, the boundary conditions also modify at every next time step. However, the solution procedure in both the aforementioned cases stays less hectic than those involving the spatial non-similarity, dealt in the previous two Chapters.

Table 11.1 Values of the coefficient of skin-friction due to [11]

K	s	M	$\tau = 1.5\,\pi$	$\tau = 5.5\,\pi$	$\tau = 9.5\,\pi$
0.0	1.0	12.0	11.678656	11.678707	11.678656
0.2			5.523296	5.523371	5.523257
0.5			−3.899067	−3.899268	−3.899162
0.8			−11.674383	−11.676506	−11.676116
1.0			−15.617454	−15.624607	−15.624963
0.2	0.5		5.322161	5.322193	5.322173
	1.0		5.523296	5.523371	5.523257
	2.0		6.087060	6.087031	6.087156
	3.0		6.769261	6.768992	6.769294
	4.0		7.497932	7.406924	7.496870
	5.0		8.232954	8.229085	8.228996
	1.0	5.0	2.323502	2.323551	2.323548
		7.0	3.278018	3.278005	3.278123
		9.0	4.197624	4.197771	4.197733
		12.0	5.423296	5.523371	5.523257
		15.0	6.791323	6.791301	6.791278

11.2 Axially Symmetric Unsteady Non-similar Flows

The unsteady non-similar flow due to a stretching disk follows similarly to the two-dimensional case because of the previously determined similarity between the disk flow and the two-dimensional flow. The case of a stretching cylinder follows also in a, somehow, similar manner but with a little difference in the governing equations because of the presence of transverse curvature parameter. Different from the planner case, the axisymmetric unsteady flow has not been studied any frequently. In this case too, the analogy of semi-similarity persists in the cases when the spatial dependence of the wall velocity follows the similarity criterion of the corresponding self-similar flow. As a consequence of it, the resulting equations also come out of the similar form as did in the previous planner cases. For an unsteady Crane's flow due to an impulsively started stretching cylinder, the governing equations are those given in Eqs. (2.13) and (2.14) subject to the initial and boundary conditions

$$\left.\begin{array}{l} \text{at } t \leq 0: \; u = v = 0, \; \forall \, z, r \\ \text{at } t > 0: \; \left\{ \begin{array}{ll} u = az, \; v = 0, & \text{at } r = R \\ u = 0, & \text{at } r = \infty \end{array} \right. \end{array} \right\}. \tag{11.12}$$

The so-called semi-similarity transformations of this problem come directly in a combination of the similarity transformations of the corresponding self-similar steady flow and those of the famous Rayleigh's problem following the Williams and Rhyne's [1] formulation. The similarity transformations for the steady case are given in Chap. 6 in dimensionless form. In view of these transformations, the similarity variables for the present unsteady problem are constructed (due to [1]) as

$$\eta = \frac{r^2 - R^2}{2R}\sqrt{\frac{a}{\nu\xi}}, \; \psi = \sqrt{a\nu\xi}\, Rzf\,(\xi, \eta), \; \xi = 1 - e^{-\tau}; \tau = at. \tag{11.13}$$

The stream function $\psi\,(r, z, t)$ is related to the velocity components u and v as $ru = \frac{\partial \psi}{\partial r}, rv = -\frac{\partial \psi}{\partial z}$ due to which the equation of continuity (Eq. 2.13) is satisfied identically and Eq. (2.14) transforms as

$$\begin{aligned} \xi\left(\left(\frac{\partial f}{\partial \eta}\right)^2 - f\frac{\partial^2 f}{\partial \eta^2}\right) &= \frac{\partial}{\partial \eta}\left[\left(1 + 2\kappa\sqrt{\xi}\eta\right)\frac{\partial^2 f}{\partial \eta^2}\right] \\ &\quad + (1 - \xi)\left(\frac{1}{2}\eta\frac{\partial^2 f}{\partial \eta^2} - \xi\frac{\partial^2 f}{\partial \eta \partial \xi}\right) \end{aligned} \tag{11.14}$$

Similar to Eq. (11.4), the above equation also recovers the Rayleigh's flow at $\xi = 0$ and the steady (Crane's) flow due to a uniformly stretching cylinder at $\xi = 1$. Based upon this reasoning, the solution of Eq. (11.14) is equally applicable to the

small time as well as to the large time scenarios. The boundary conditions in terms of transformed variables are given by

$$f(0,\xi)=0,\ \left.\frac{\partial f}{\partial \eta}\right|_{\eta=0}=1,\ \left.\frac{\partial f}{\partial \eta}\right|_{\eta=\infty}=0. \tag{11.15}$$

This problem has already been studied in detail by Munawar et al. [12] including the heat transfer phenomena for the cases of prescribed surface temperature (PST) and prescribed heat flux (PHF). Analytic and numerical solutions were obtained due to the HAM and the finite difference numerical scheme, respectively. The HAM solution for the dimensionless stream function is obtained in the form of the series [12]

$$f(\xi,\eta)=\sum_{k=0}^{\infty}\sum_{m=0}^{\infty}\sum_{l=0}^{\infty}\alpha_{m,l}^{k}\xi^{k}\eta^{l}\mathrm{e}^{-m\eta},$$

where the $\alpha_{m,l}^{k}$ are the constant coefficient of the series and m,l,k are the involved indices. The initial solution and the linear operator were chosen of the form

$$f_0(\xi,\eta)=1-\mathrm{e}^{-\eta}\quad\text{and}\quad L=\frac{\partial}{\partial\eta^3}-\frac{\partial}{\partial\eta},$$

respectively.

In the numerical solution, the authors of [12] utilized the finite difference scheme by approximating the partial derivatives by the finite differences of the form

$$\frac{\partial f}{\partial\bar{\eta}}=\frac{f_{j+1}-f_{j-1}}{2\Delta\bar{\eta}},\frac{\partial^2 f}{\partial\bar{\eta}^2}=\frac{f_{j+1}-2f_j+f_{j-1}}{(\Delta\bar{\eta})^2},$$
$$\frac{\partial^3 f}{\partial\bar{\eta}^3}=\frac{f_{j+2}-3f_{j+1}+3f_j-f_{j-1}}{(\Delta\bar{\eta})^3},\frac{\partial f}{\partial\xi}=\frac{f_{j+1}-f_j}{\Delta\xi}$$

where $\bar{\eta}=\frac{1}{1+\eta}$ which transforms the semi-infinite spatial domain $[0,\infty)$ to a bounded interval $[0,1]$ in order to facilitate the numerical computations. The accuracy of the two solutions is shown in Table 11.2 where the analytic and numerical results reported by [12] have been compared. An excellent agreement can be seen in the two solutions. The velocity graphs for different values of the time variable τ are shown in Fig. 11.3. Analogous to Fig. 11.1, with the passage of time the flow develops within the boundary-layer and attains the steady state for sufficiently large values of τ. The coefficient of skin-friction in this case is given by

$$\frac{1}{2}Re_xC_f=\frac{1}{\xi}\left.\frac{\partial^2 f}{\partial\eta^2}\right|_{\eta=0}. \tag{11.16}$$

Table 11.2 Comparison between the analytic and numerical solutions for different values of the curvature parameters κ and ξ, at the 13th-order Padé approximation

$f''(0,\xi)$				
κ	HAM results $\xi = 0.2$	Numerical results $\xi = 0.2$	HAM results $\xi = 0.4$	Numerical results $\xi = 0.4$
0.0	−0.65611	−0.65652	−0.74578	−0.74578
0.2	−0.69813	−0.69910	−0.80232	−0.80251
0.5	−0.75824	−0.75816	−0.88255	−0.88260
1.0	−0.85228	−0.85233	−1.00695	−1.00713
1.5	−0.94979	−0.94983	−1.12328	−1.12331
2.0	−1.02509	−1.02515	−1.42200	−1.42200

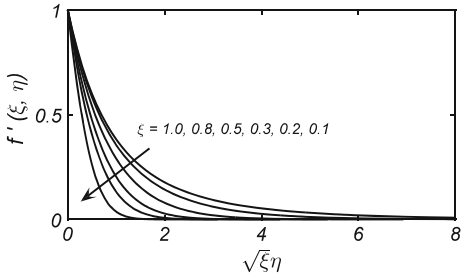

Fig. 11.3 Velocity profile at different ξ values

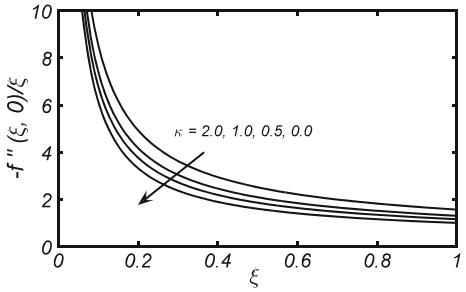

Fig. 11.4 Coefficient of skin-friction against ξ for different κ

The variation of $\frac{1}{2}Re_xC_f$ against ξ for different values of the curvature parameter κ is shown in Fig. 11.4. Obviously, the skin-friction varies quite rapidly for small values of time τ and stabilizes for sufficiently large values of time. The transition time is that which is taken by the impulsively started fluid in establishing the fully developed flow within the boundary-layer. The results of heat transfer phenomena have intentionally been disregarded, and the interested reader is referred to follow Ref. [12] in this regard.

11.2.1 The Case of Oscillatory Stretching

The case of oscillatory stretching rate of the linear stretching velocity of the cylinder's surface, for which the steady flow admits a self-similar solution, follows also in the same manner as does the corresponding planner case. In this case, the rate of stretching is assumed to be a periodic function of sin or cos as considered in the previous Section. Different from the previous case, the oscillatory rate of stretching wall velocity may also be taken as

$$u_w(z,t) = a(1+\epsilon\, cos\, \omega t)z. \tag{11.17}$$

This particular form of the wall velocity has also been investigated by Munawar et al. [13]. In this case, the momentum Eq. (2.14) comes out of the form

$$\left(\frac{\partial f}{\partial \eta}\right)^2 - f\frac{\partial^2 f}{\partial \eta^2} = \kappa \frac{\partial}{\partial \eta}\left((1+\eta)\frac{\partial^2 f}{\partial \eta^2}\right) - St\frac{\partial^2 f}{\partial \eta \partial \tau}, \tag{11.18}$$

and the equation of continuity (2.13) satisfies identically. The so-called semi-similarity transformations, as utilized by [13], read as

$$\eta = \left(\frac{r}{R}\right)^2 - 1,\ \psi = azR^2 f(\eta,\tau),\ \tau = \omega t, \tag{11.19}$$

due to which the boundary conditions in terms of new variables are given by

$$\left.\frac{\partial f}{\partial \eta}\right|_{\eta=0} = 1+\epsilon cos\, \tau, f(0,\tau) = 0,\ \left.\frac{\partial f}{\partial \eta}\right|_{\eta=\infty} = 0, \tag{11.20}$$

where ϵ denotes the amplitude of oscillations; for $\epsilon = 0$ (no oscillations), the case of steady flow is recovered. The coefficient of skin-friction in view of Eq. (11.19) takes the form

$$\frac{1}{2}Re_x C_f = \left.\frac{\partial^2 f}{\partial \eta^2}\right|_{\eta=0}. \tag{11.21}$$

The variation of velocity and the skin-friction coefficient due to the varying values of the Strouhal number and the parameter ϵ have been depicted in Figs. 11.5, 11.6, 11.7, 11.8, and 11.9. Clearly, upon increasing the values of amplitude parameter, the velocity increases and the amplitude of oscillations in the skin-friction graphs increases. Similar trend persists for the increasing values of the Strouhal number also. Development of the flow, for initial values of time, can obviously be seen in Figs. 11.8 and 11.9 where the coefficient of skin-friction undergoes rapid variations for small time values and established afterward.

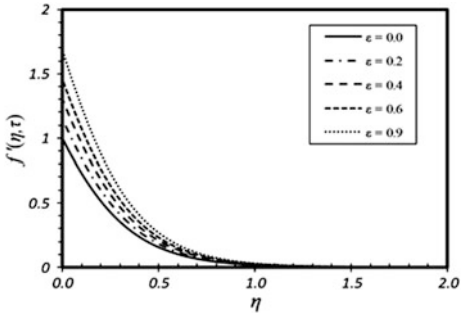

Fig. 11.5 Velocity graph against η for different ϵ

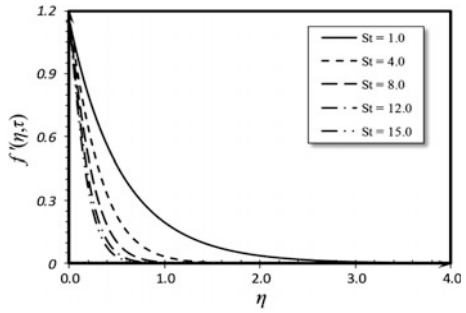

Fig. 11.6 Effect of Strouhal number *St* on velocity profile

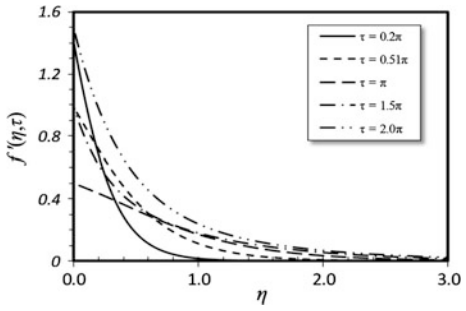

Fig. 11.7 Velocity graph at different time values

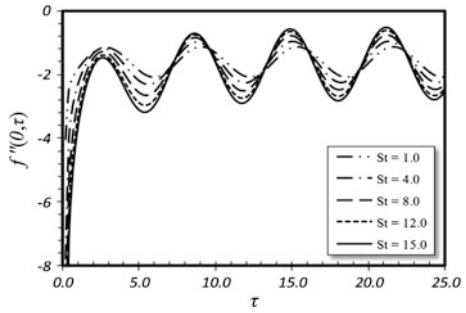

Fig. 11.8 Variation of skin-friction against τ corresponding to various values of *St*

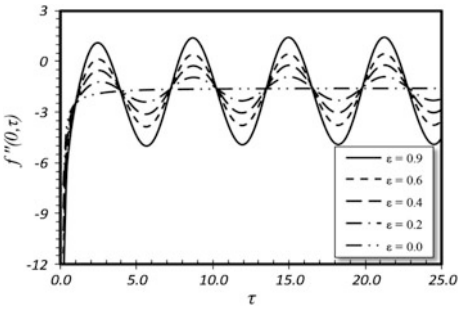

Fig. 11.9 Impact of amplitude parameter ϵ on the skin-friction profile

To all the problems, considered in this Chapter, the name "non-similar" flows has repeatedly been referred, whereas the literature recognizes them as the semi-similar flows. The reason behind their designation as semi-similar is that they do not depart far away from the similarity solution and finally attain the steady-state self-similar solution, particularly in the impulsively started cases. However, besides such a physical nobility, their governing equations never ever allow the reduction of three independent variables to one (the self-similar solution). Because of such a non-reducible nature of their associated manifold, they fail to fulfill the criterion of self-similarity, in general. This is the fundamental reason due to which they have been referred as the time-dependent non-similar flows. However, it has also been stated several times, in this Chapter, that these time-dependent non-similar flows are not that severe and challenging as do the spatially non-similar flows. Therefore, besides calling them the semi-similar flows, it must not be confused that they are not non-similar. Actually, they are non-similar, but the passive nature of temporal non-similarity does not take them far away from the spatially self-similar solution due to which they are commonly known as the semi-similar solutions.

References

1. J.C. Williams III, T.B. Rhyne, Boundary-layer development on a wedge impulsively set into motion. SIAM J. Appl. Math. **38**(2), 215–224 (1980)
2. K. Stewartson, On the impulsive motion of a flat plate in a viscous fluid. Quart. J. Mech. App. Math. **4**, 182–198 (1951)
3. H. Xu, S.J. Liao, Series solution of unsteady magnetohydrodynamic flows of non-Newtonian fluids caused by an impulsively stretching plate. J. Non-Newtonian Fluid Mech. **129**, 46–55 (2005)
4. S.J. Liao, An analytic solution of unsteady boundary-layer flow caused by an impulsively stretching plate. Commun. Nonlinear Sci Numer. Simulat. **11**(3), 326–339 (2006)
5. A. Mehmood, A. Ali, Unsteady boundary-layer flow due to an impulsively started moving plate. Proc. Inst. Mech. Eng. Part G: J. Aero Eng. 221, 385–390 (2007)
6. A. Mehmood, A. Ali, H.S. Takhar, T. Shah, Unsteady three-dimensional MHD boundary-layer flow due to impulsive motion of a stretching surface (Acta Mech. 146, 59–71, 2001), Acta Mech. 199, 241–249 (2008)

7. I. Ahmad, M. Sajid, T. Hayat, M. Ayub, Unsteady axisymmetric flow of a second-grade fluid over a radially stretching sheet. Comput. Math. Appl. **56**(5), 1351–1357 (2008)
8. C.Y. Wang, Q. Du, M. Miklavcic, C.C. Chang, Impulsive stretching of a surface in a viscous fluid. SIAM J. Appl. Math. **57**(1), 1–14 (1997)
9. I. Pop, T.Y. Na, Unsteady flow past a stretching sheet. Mech. Res. Commun. **23**(4), 413–422 (1996)
10. C.Y. Wang, Nonlinear streaming due to the oscillatory stretching of a sheet in a viscous fluid. Acta Mech. **72**, 261–268 (1988)
11. Z. Abbas, Y. Wang, T. Hayat, M. Oberlack, Hydromagnetic flow in a viscoelastic fluid due to the oscillatory stretching surface. Int. J. Non-Linear Mech. **43**, 783–793 (2008)
12. S. Munawar, A. Mehmood, A. Ali, Time-dependent flow and heat transfer over a stretching cylinder. Chin. J. Phys. **50**(5), 828–848 (2012)
13. S. Munawar, A. Mehmood, A. Ali, Unsteady flow of viscous fluid over the vascillate stretching cylinder. Int. J. Numer. Methods Fluids **70**, 671–681 (2012)